DO COMMONLY USED B-VALUES YIELD ACCURATE APPARENT KURTOSIS VALUES?

T. Kuder[1], B. Stieltjes[2], W. Semmler[1], and F. B. Laun[1]
[1]Medical Physics in Radiology, German Cancer Research Center, Heidelberg, Germany, [2]Quantitative Imaging-based Disease Characterization, German Cancer Research Center, Heidelberg, Germany

Introduction

The diffusion restrictions present in biological tissue result in deviations from the Gaussian propagator shape, which can be quantified using the apparent kurtosis K_{app} [1]. K_{app} is defined by eq. 1, where $<\phi^n>$ is the expectation value of the n-th power of the spin phase, and it appears in the expansion of the logarithmic signal in powers of b (eq. 2).

$$K_{app} = \langle \phi^4 \rangle \big/ \langle \phi^2 \rangle^2 - 3 \quad (1); \qquad \ln[S(b)/S(0)] = -b\,D_{app} + b^2 D_{app}^2\,K_{app}/6 + A\,b^3 + B\,b^4 + \ldots \quad (2);$$

In practice, to measure the kurtosis, the expansion (eq. 2) is terminated after the quadratic summand and the resulting polynomial is fitted to the signal acquired at different b-values [1]. The kurtosis obtained this way is named $K_{app,fit}$. In clinical applications, the maximum b-value b_{max} is typically chosen such that $b_{max}D_{app}$ ranges from 1 to 2. Since it is not clear to date whether this choice of maximal b-values is appropriate, the aim of this work was to verify that question for different model geometries and in phantom experiments.

Methods

For the simulation of diffusion inside closed geometries (slab, cylinder, sphere), the multiple correlation function approach [2] was used, which allows a very accurate signal calculation with short computation times. The number of eigenvalues of the Laplace operator used for the calculation was 100. Bipolar gradients of duration T were chosen, with the gradient amplitude g for $0 \le t \le T/2$ and $-g$ for $T/2 < t \le T$. The results were substantiated by Monte Carlo random walk simulations. For open geometries, Monte Carlo simulations were used simulating the random walk of particles in the space between impermeable cylinders with different packing distributions: cubic, hexagonal and hexagonal with holes; and with different packing densities. In the case of a collision with the confining geometry, the rest of the step was executed starting at the collision point with an appropriately reduced step size. In all simulations, the time T was varied in the range from 5 ms to 150 ms. The free diffusion constant was set to D = 2 µm²/ms, the thickness of the slab to 15 µm, the diameters of the sphere and of the cylinders to 7.5 µm. For different b_{max}-values, the signal was calculated for 20 equidistant b-values ranging from 0 to b_{max} and the kurtosis $K_{app,fit}$ was obtained by fitting eq. 2. In addition, K_{app} was directly calculated with eq. 1.

Phantom datasets were acquired on a 1.5 T MR scanner (Avanto, Siemens) using a standard twice refocused spin echo EPI diffusion sequence (TR=4 s, TE=144 ms, voxel size 2.5×2.5×5 mm³, FOV 320×190 mm², 1 gradient direction orthogonal to the fibers, 32 averages, 18 b_{max}-values ranging from 1500 to 10 000 s/mm², 16 equidistant b-values for each b_{max}-value ranging from 0 to b_{max}). The phantoms consist of parallel fibers (radius 7.5 µm) with diffusing water between them [3].

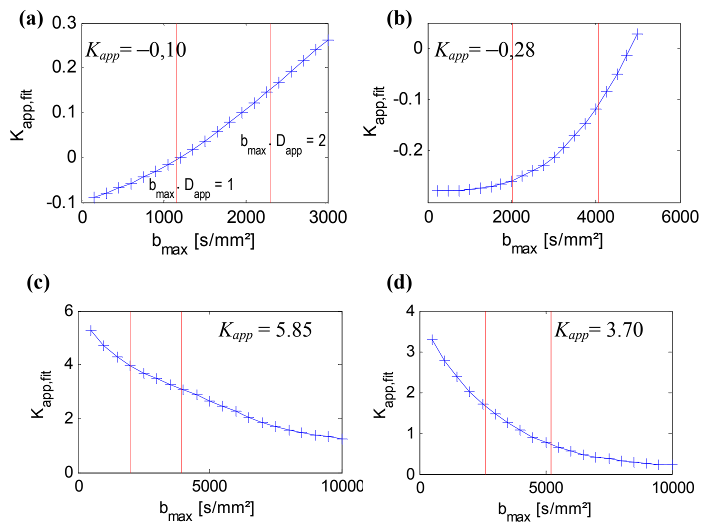

Fig. 1: Dependence of the kurtosis $K_{app,fit}$ on b_{max} simulated for different geometries: diffusion inside cylinder for (a) T = 16 ms and (b) T = 28 ms; diffusion between cylinders for (c) cubic packing (T = 40 ms) and (d) hexagonal packing with holes (T = 96 ms). Red lines indicate typical b-values used in vivo. For these b-values a strong deviation of $K_{app,fit}$ from K_{app} is observed in most cases.

Results

In almost all simulations, applying b-values such that $b_{max}D_{app}$ is between 1 and 2 results in substantial deviations of $K_{app,fit}$ from K_{app}. Fig. 1 shows four exemplary graphs for diffusion inside cylinders (a,b) and between cylinders (c,d), demonstrating three different possible dependencies of $K_{app,fit}$ on b_{max}. In Fig. 1c and 1d, $K_{app,fit}$ is highly *underestimated*, for instance by the factor 5.2 at $b_{max}D_{app}$ = 2.

In Fig. 1b, in which $K_{app,fit}$ is *overestimated*, a rather exceptional case is shown: There is only a weak dependence on b_{max} for $b_{max}D_{app} < 1$.

In Fig. 1a, for $b_{max}D_{app} > 1$, even the *sign* of $K_{app,fit}$ is different from that of K_{app}. In general, the influence of b_{max} on $K_{app,fit}$ strongly depends on geometry and on the time T, but in all cases, $K_{app,fit}$ converged to K_{app} in the limit of very small b_{max} .

$K_{app,fit}$ as determined in the phantom is shown in Fig. 2. As in the simulations, $K_{app,fit}$ exhibits a strong influence of b_{max}. The fact, that Fig. 2 is qualitatively similar to Fig. 1c,d, can be understood by considering the similarity of the phantom geometry and the geometry used for the simulations.

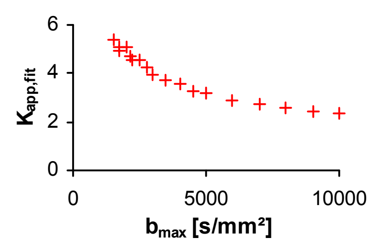

Fig. 2: Kurtosis measured orthogonal to the fibers of a diffusion phantom. $K_{app,fit}$ strongly depends on b_{max}, similar to the simulations in Fig. 1 c,d.

Discussion

At the b-values typically used in vivo ($b_{max}D_{app} > 1$), $K_{app,fit}$ mostly deviates strongly from K_{app} for the model geometries used in the simulations. Consequently, the measured kurtosis $K_{app,fit}$ is a mixture of K_{app} and higher orders in the expansion (eq. 2). This strong influence of higher powers of b also can be observed in phantom datasets. Initial measurements in the human brain suggest that the higher order contributions are also relevant for in vivo measurements. To reduce the influence of the higher order terms, measuring at very low b-values would be desirable. Then, however, the signal drop and the curvature of the logarithmic signal are often insufficient for a stable K_{app}-fit. A potential remedy allowing to measure K_{app} experimentally might be to acquire a $K_{app,fit}$ as a function of b_{max} and to extrapolate this curve to small b-values.

References

[1] Jensen et al. MRM 2005; [2] D. Grebenkov, Concepts Magn Reson Part A 2008; [3] Laun et al. MRI 2009